iScience

CellPress
OPEN ACCESS

Article

Mass burial genomics reveals outbreak of enteric paratyphoid fever in the Late Medieval trade city Lübeck

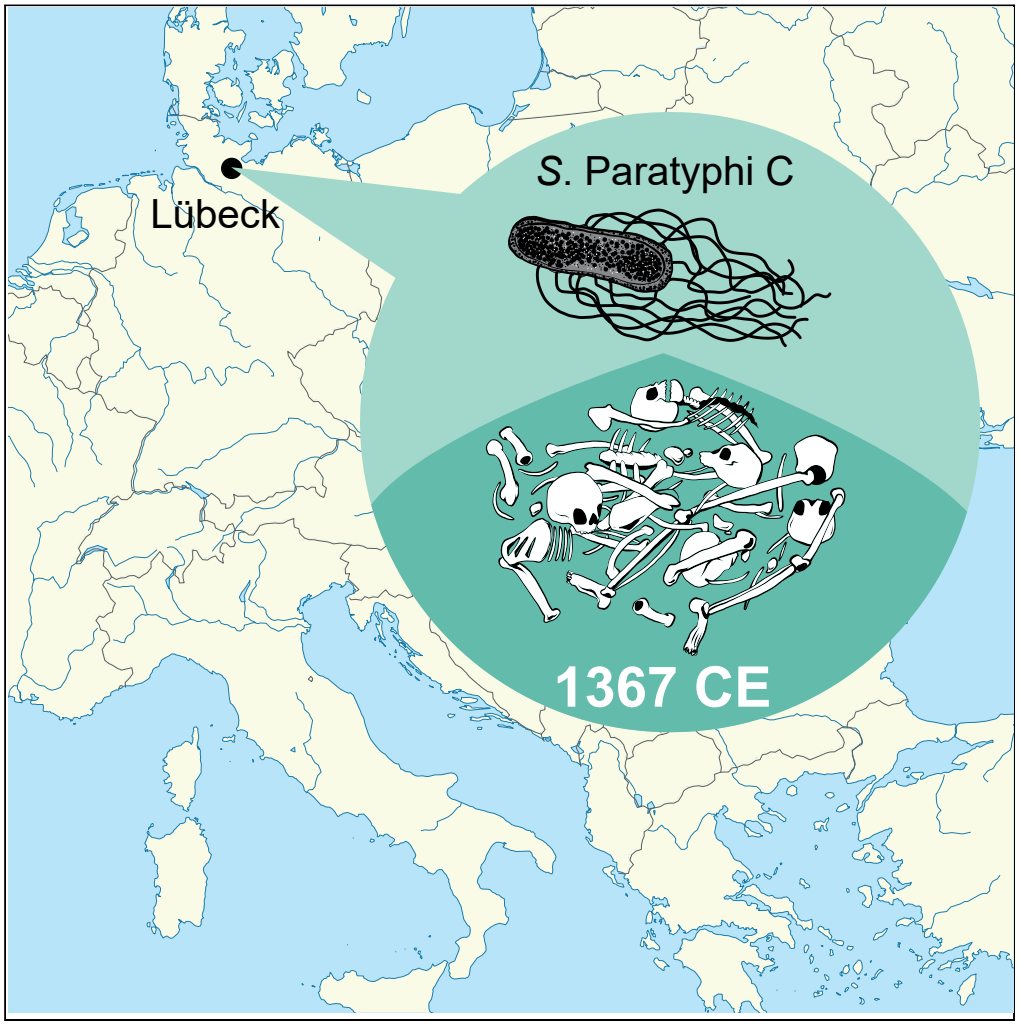

Magdalena Haller, Kimberly Callan, Julian Susat, ..., Dirk Rieger, Almut Nebel, Ben Krause-Kyora

b.krause-kyora@ikmb.uni-kiel.de

Highlights

Salmonella enterica Paratyphi C detected in remains from a mass burial in Lübeck

Outbreak of enteric paratyphoid fever likely occurred in 1367 CE

Pathogen genomes showed close similarity to a strain from Norway (1200 CE)

Haller et al., iScience 24, 102419
May 21, 2021
https://doi.org/10.1016/j.isci.2021.102419

iScience

CellPress
OPEN ACCESS

Article

Mass burial genomics reveals outbreak of enteric paratyphoid fever in the Late Medieval trade city Lübeck

Magdalena Haller,[1] Kimberly Callan,[1,2] Julian Susat,[1] Anna Lena Flux,[3] Alexander Immel,[1] Andre Franke,[1] Alexander Herbig,[4] Johannes Krause,[4] Anne Kupczok,[5,6] Gerhard Fouquet,[7] Susanne Hummel,[3] Dirk Rieger,[8] Almut Nebel,[1,9] and Ben Krause-Kyora[1,9,10,*]

SUMMARY

Medieval Europe was repeatedly affected by outbreaks of infectious diseases, some of which reached epidemic proportions. A Late Medieval mass burial next to the Heiligen-Geist-Hospital in Lübeck (present-day Germany) contained the skeletal remains of more than 800 individuals who had presumably died from infectious disease. From 92 individuals, we screened the ancient DNA extracts for the presence of pathogens to determine the cause of death. Metagenomic analysis revealed evidence of *Salmonella enterica* subsp. *enterica* serovar Paratyphi C, suggesting an outbreak of enteric paratyphoid fever. Three reconstructed *S.* Paratyphi C genomes showed close similarity to a strain from Norway (1200 CE). Radiocarbon dates placed the disease outbreak in Lübeck between 1270 and 1400 cal CE, with historical records indicating 1367 CE as the most probable year. The deceased were of northern and eastern European descent, confirming Lübeck as an important trading center of the Hanseatic League in the Baltic region.

INTRODUCTION

In the High and Late Middle Ages, European settlements of all sizes were repeatedly struck by outbreaks of infectious diseases. Some of them reached epidemic proportions such as smallpox (Duggan et al., 2016), leprosy (Krause-Kyora et al., 2018a; Schuenemann et al., 2013, 2018), or the second plague pandemic that started with the Black Death (Bos et al., 2011; Haensch et al., 2010; Spyrou et al., 2016, 2019). Medieval chronicles generally referred to epidemics as "pestis" or "pestilentiae", regardless of the causative pathogen responsible (Kahlow 2007). Increasing trade and mobility played an important role in spreading pathogens along cross-country and maritime routes throughout the continent (Yue et al., 2017). One of the most important medieval commercial networks was the Hanseatic League, which dominated the northern European and Baltic maritime trade from the 13th to the 16th century (Dollinger and Krabusch, 1998). At its center was the city of Lübeck in present-day Germany, a wealthy and influential trading hub on the Baltic Sea (Benedictow, 2017; Singman, 1999) (Figure 1A). In 1226 CE, the Heiligen-Geist-Hospital ("Hospital of the Holy Ghost", HGH) was established there, which was dedicated to the care and welfare of the elderly (Lütgert, 2002). The large building complex still exists today and is currently in use as a retirement home as well as a museum. In 1989, construction works on the southern walls of the hospital revealed a mass burial site nearby (Figure 1B), containing the remains of more than 800 individuals from the Late Middle Ages (Lütgert, 2002; Prechel, 1996, 2002) (Figures 1C and 1D). Based on archaeological evidence and the lack of traumatic lesions on the bones, the dead were assumed to represent victims of an epidemic event, most likely of the Black Death, as the plague was reported to have affected Lübeck successively, first in 1350 CE (Koppmann, 1899) and later again in 1359 CE (Koppmann, 1884). However, these outbreaks were followed by at least four more pestilences of unclear etiology in the 14th century (Koppmann, 1884).

In order to identify the infectious agent that led to the death of the individuals buried next to the HGH in Lübeck, we screened the skeletal remains of 92 individuals from this site for the presence of pathogens. We found evidence of an infection with the bacterium *Salmonella enterica* subsp. *enterica* serovar Paratyphi C

[1]Institute of Clinical Molecular Biology, Kiel University, 24105 Kiel, Germany

[2]Present address: Department of Genetics, Harvard Medical School, Boston, MA 02115, USA

[3]Department of Historical Anthropology and Human Ecology, University of Göttingen, 37073 Göttingen, Germany

[4]Max Planck Institute for the Science of Human History, 07743 Jena, Germany

[5]Genomic Microbiology Group, Institute of General Microbiology, Kiel University, 24118 Kiel, Germany

[6]Bioinformatics Group, Wageningen University & Research, 6708 PB Wageningen, The Netherlands

[7]Historical Seminar, Faculty of Arts and Humanities, Kiel University, 24118 Kiel, Germany

[8]Department of Archaeology, Hanseatic City of Lübeck Historical Monuments Protection Authority, 23539 Lübeck, Germany

[9]These authors contributed equally

[10]Lead contact

*Correspondence: b.krause-kyora@ikmb.uni-kiel.de

https://doi.org/10.1016/j.isci.2021.102419

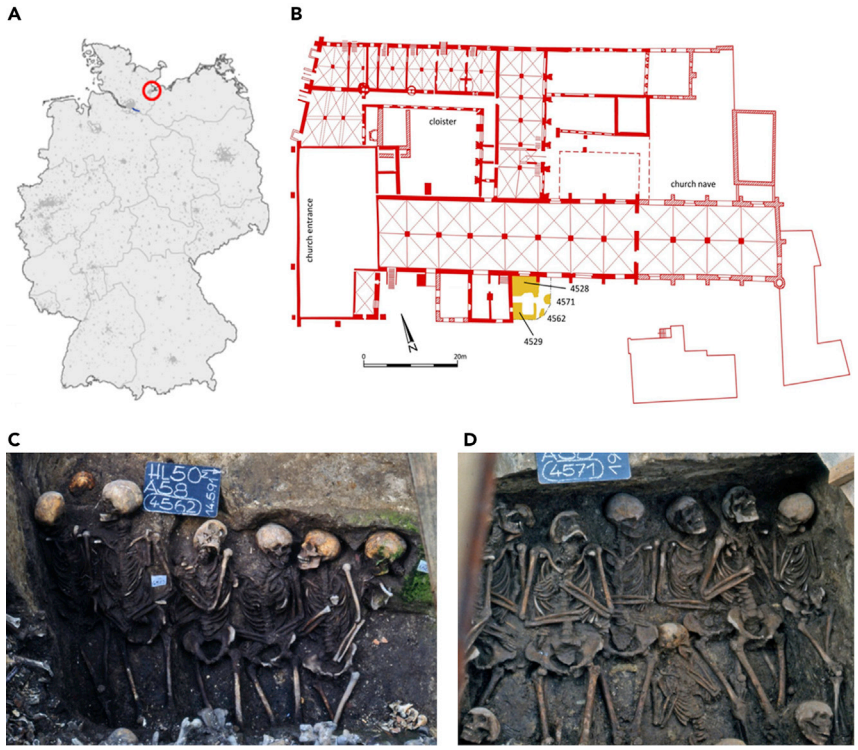

Figure 1. The excavation site of the Heiligen-Geist-Hospital (HGH) in Lübeck

(A) Location of Lübeck in present-day northern Germany.

(B–D) (B) Plan of the HGH building complex. The mass graves 4528 and 4529 and the two multiple burial pits 4562 and 4571 are indicated. All *S.* Paratyphi C-positives were found in the pits 4562 (C) and 4571 (D).

(*S.* Paratyphi C) in eight individuals, suggesting an outbreak of enteric paratyphoid fever that afflicted the city of Lübeck in the late 14th century.

RESULTS

In this study, we analyzed 92 individuals excavated from the HGH mass burial site in Lübeck. The remains were obtained from four archaeological contexts, i.e., from two mass graves (4528, *n = 29* and 4529, *n = 11*) and two smaller pits (4562, *n = 13* and 4571, *n = 39*; Figures 1C and 1D). We performed radiocarbon dating which placed all four contexts in the same time range from 1270 to 1400 cal CE (Table S1 and Figure S1). However, based on a coin found *in situ* (4528), the period of use of the mass graves could be narrowed down to 1340–1370 CE. The two smaller pits stratigraphically cut into the mass grave contexts and are therefore considered younger (Prechel, 2002).

We extracted ancient DNA (aDNA) from teeth and/or bones of all 92 individuals following established guidelines for the work with tiny amounts of fragmented DNA (Cooper and Poinar, 2000). All procedures were conducted in dedicated aDNA clean rooms. Blank controls that were included in each experimental step were always negative. Short tandem repeat profiles at seven loci were generated as an additional authentication criterion and to avoid double sampling (Table S2).

Metagenomic screening

First, all metagenomic aDNA extracts were screened for bacterial and viral pathogens using an established in-house pipeline (Krause-Kyora et al., 2018a, 2018b; Susat et al., 2020). Ten data sets were observed to align to the taxonomic node of *S. enterica* subsp. *enterica*, based on a threshold of at least 300 reads per sample aligning to *S. enterica* from an initial sequencing depth of 2–54 million reads per sample (Table S3). The sequencing reads were then competitively mapped to a multi-sequence reference comprising the

Table 1. Sequencing and mapping statistics of the eight *S.* Paratyphi C-positive samples from the HGH in Lübeck

Sample	Context	Pre-processed reads prior to mapping (n)	Unique reads mapped to *S.* Paratyphi C (n)	Quality filtered endogenous DNA (%)	Mean coverage	Percentage of genome covered at least 1-fold	Percentage of genome covered at least 2-fold
HGH-1429	4571	544,611,092	291,107	0.42	4.05	85.8	75.06
HGH-1510	4571	15,763,343	473	0.003	0.0057	0.56	0.01
HGH-1558	4571	641,527,718	229,593	0.293	2.99	82.11	64.07
HGH-1579	4562	533,324,715	41,228	0.04	0.79	50.2	19.51
HGH-1599	4571	6,435,352	459	0.008	0.0065	0.65	0.01
HGH-1600	4571	530,411,412	562,392	0.173	6.73	96.96	95.62
HGH-1607	4562	184,903,636	13,219	0.035	0.12	10.65	1.03
HGH-1638	4571	548,078,315	18,361	0.015	0.19	16.26	2.11

Data sets were mapped to the reference genome of *S.* Paratyphi C RKS4594 (NC_012125).

complete genomes of 15 different serovars that represent the modern diversity of *S. enterica* (Table S4). In eight of the ten data sets, *S.* Paratyphi C was the reference with the highest number of aligned reads. For two samples (HGH-1458, HGH-1699), the aligned reads were subsequently identified as false positives. The *S.* Paratyphi C classifications in the other eight samples were confirmed through a taxa-specific mapping score (see methods; Table S3) that was developed analogously to the mapping score described in a study of *Yersinia pestis* (*Y. pestis)* (Andrades Valtueña et al., 2017). Additionally, we used the tool MaltExtract (Hübler et al., 2019) to verify the findings (Table S3). Based on these criteria, we identified eight positive samples (HGH-1429, HGH-1510, HGH-1558, HGH-1579, HGH-1599, HGH-1600, HGH-1607, HGH-1638; Table 1) for which additional 185 to 642 million reads were generated to facilitate genome reconstruction. The obtained sequencing reads were then aligned to the reference genome of *S.* Paratyphi C RKS4594 (NC_012125), and consensus sequences with a 2-fold genome-wide coverage of up to 96% were constructed (Table 1). All samples displayed typical damage patterns for both ancient bacterial and human DNA (Figures S2 and S3).

It is noteworthy that the *S.* Paratyphi C-positive results were only observed in human remains from the multiple burial pits 4562 ($n = 2$) and 4571 ($n = 6$) but not in skeletons from the mass graves 4528 and 4529 (Table S3). In previous publications, the plague was assumed to have caused the death of the individuals buried next to the HGH (Prechel, 1996, 2002). However, in our metagenomic screening of the 92 aDNA extracts, there was no evidence of *Y. pestis* reads.

Phylogenetic reconstruction

Next, we computed a Bayesian phylogenetic tree based on a multi-variant alignment, including three genomes with high coverage from this study (HGH-1429, HGH-1558, HGH-1600; Table 1) as well as nine ancient (Key et al., 2020; Vågene et al., 2018; Zhou et al., 2018) and 123 modern *S. enterica* subsp. *enterica* genomes (Alikhan et al., 2018; O'Leary et al., 2016; Zhou et al., 2020). The consensus sequences of the remaining five samples from Lübeck were not considered for phylogenetic reconstruction due to low coverage (a 1-fold coverage below 51%; Table 1). All ancient and modern *S.* Paratyphi C strains formed a single clade in the tree, supported by a posterior probability of 1 (Figure 2). The three genomes from Lübeck clustered together. They differed from each other only in up to four single-nucleotide polymorphisms (SNPs); this variation probably reflects the micro-diversity within an outbreak (Table S5). The SNP effect analysis showed that none of the four variants had an influence on virulence or function. Furthermore, the three HGH genomes were similar to two previously published ancient *S.* Paratyphi C genomes, those from Ragna (Norway 1200 CE) (Zhou et al., 2018) and Tepos (Mexico 1545 CE) (Vågene et al., 2018) (Figure S4).

Population genetic analyses

In a second approach, we analyzed the 92 metagenomic sequences with respect to the presence of human DNA. Fifty-three data sets were of sufficient quality for population genetic analyses (Table S3). In a principal component analysis, the individuals from medieval Lübeck grouped together and showed genetic similarities to modern populations from Scandinavia and the Baltic region, including northern Germany (Figures 3

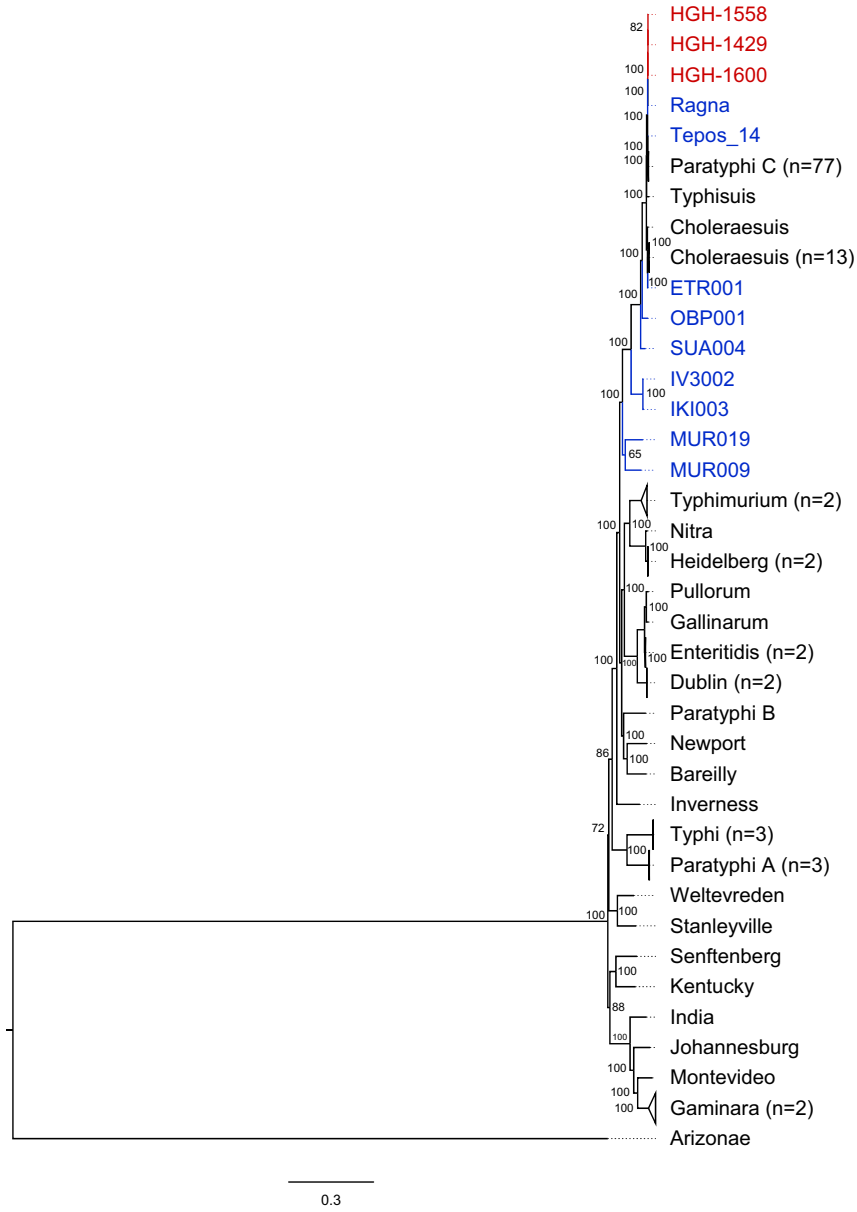

Figure 2. Phylogenetic relationship of ancient and modern *Salmonella enterica* genomes

Bayesian phylogenetic tree of three genomes from the HGH mass burial site in Lübeck (red), nine ancient (blue), and 123 modern (black) *S. enterica* genomes. *S. enterica* subsp. *arizonae* RKS2983 is used as out-group. Branches of the same serovars are collapsed, and the number of combined reference genomes is given in brackets. Nodes are labeled with posterior probabilities estimated by MrBayes. Branch lengths correspond to the number of substitutions per site. An enlarged section of the three HGH Lübeck genomes as well as those from Ragna and Tepos is provided in Figure S4.

and S5). Further, f3 statistics revealed affinities between Lübeck and populations from northern and eastern Europe (Figure S6). Mitochondrial (mt) haplogroups could be determined in 52 individuals. The mtDNA distribution in Lübeck was similar to that observed in other central and northern European populations, with haplogroups H and U being the most abundant (Table S3).

DISCUSSION

The Late Medieval mass burial site next to the HGH in Lübeck comprised the skeletons of more than 800 individuals that had been interred in two mass graves and two smaller burial pits, probably in the course of

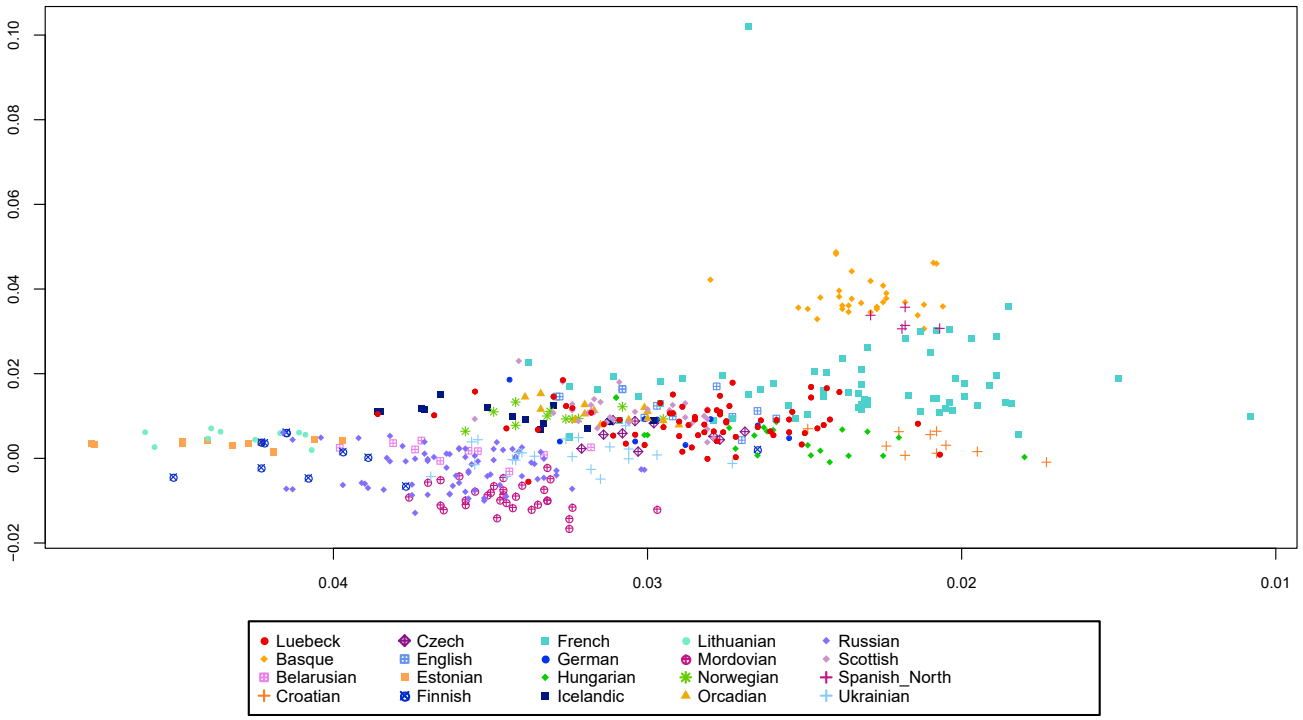

Figure 3. Population genetic analysis

Principal component analysis (PCA) of HGH individuals (red circles) from Lübeck in the context of 19 modern-day European populations. A PCA with a larger set of reference populations is shown in Figure S5.

different disease outbreaks. Our pathogen screening revealed *Salmonella enterica* subsp. *enterica* serovar Paratyphi C in skeletal remains from the two burial pits, indicating the highly contagious enteric paratyphoid fever as the cause of death. However, we could not detect any traces of *S. enterica* or *Y. pestis* in the two mass graves.

Our radiocarbon dates (1270–1400 cal CE; Table S1) and the coin (1340–1370 CE) place all four contexts in the second half of the 14th century. Several consecutive epidemics were recorded to have affected the city of Lübeck in this period. The first in 1350 CE and the second in 1359 CE are usually attributed to the Black Death that was responsible for a very high death toll in all cities on the coast of northern Germany (Koppmann, 1884). The large number of corpses in the mass graves suggests that they were the victims of one or both plague waves (Prechel, 1996, 2002), though we did not find genetic traces of *Y. pestis*.

As the two pits were stratigraphically younger than the mass graves (Lütgert, 2002; Prechel, 2002), we hypothesize that the 120 deceased in the two pits had succumbed to one of the later dated pestilences, i.e., between 1360 and 1400 CE. The archaeological context indicates that the pits were refilled quickly, which suggests that all the individuals had died from the same disease, paratyphoid fever, within a short time. This scenario is supported by our detection rate (8 *S.* Paratyphi C-positives in 52 remains from the two pits) that is remarkably high for ancient pathogen diagnostics.

The city chronicles mentioned a third epidemic of unknown cause in 1367 CE, which was limited to Lübeck only (Koppmann, 1899; Ibs, 1994). The clinical manifestation of paratyphoid fever would be consistent with such a localized event. Lübeck was a clean city by the standards of the time and had invested in eliminating health hazards, for example, by introducing separate sewage and drinking water systems (Grabowski and Schmitt, 1993; Lüdecke, 1980). An outbreak of paratyphoid fever therefore seems somewhat surprising. But *S.* Paratyphi C bacteria, which grow in the intestines and blood, are easily spread via water or food contaminated with the feces of an infected individual. In many cases, transmission occurs when active or asymptomatic carriers (super-spreaders) do not wash their hands before preparing or

handling food (Bhan et al., 2005; Crump and Mintz, 2010; Sánchez-Vargas et al., 2011). Because the dead were buried next to the HGH, these premises appear to be a possible hotspot of infection. However, the HGH was not a hospital in the modern sense of the word, but rather a social institution managed by the city council providing housing, food, and care for the more affluent elderly who bought the prerogative to reside in the HGH. It thus resembled more a present-day retirement or nursing home. About 51% of the skeletons in the two smaller burial pits represented individuals younger than 40 years (Prechel, 1996) who were unlikely to have lived in an old age home. Besides, the HGH maintained its own regular graveyard in the vicinity. It can therefore be assumed that the majority of the dead in the pits, especially the younger ones, were not residents of the HGH. A paratyphoid fever outbreak that claimed 120 lives from all age groups (Prechel, 1996) must have affected many households. Due to the lack of written or archaeological evidence, we do not know from where the paratyphoid fever emanated or how it spread. But as Lübeck was densely populated and there was no gentrification of residential districts (Hammel-Kiesow, 2006), the outbreak probably affected people of all social strata, including wealthier citizens. This scenario is in agreement with the city chronicles which mentioned that a large proportion of the affluent population was killed in the outbreak of 1367 CE (Koppmann, 1884). However, the latter had their own cemeteries outside the city (Koppmann, 1899), so it was unlikely that they would be interred in a mass burial. In contrast, as evidenced by the different mass graves at the HGH, its unconsecrated grounds were apparently repeatedly used for the disposal of corpses which accumulated rapidly during epidemics and must primarily have come from people who were not wealthy enough for a proper burial in the established cemeteries. In any case, the results of our population genetic analyses showed that the dead represented a varied group of people of northern and eastern European descent. This finding is compatible with the role of Lübeck as an important trading center of the Hanseatic League. The city is often referred to as "The Queen of the Hansa", attracting merchants, sailors, and workers from all over the Baltic region. Due to the Hanseatic trade and the institutionalized trading stations of the Hanseatic Merchant in Bergen (Norway) and Novgorod (Russia), Lübeck was a melting pot of very diverse people (Dollinger and Krabusch, 1998; Graβmann, 2005).

S. Paratyphi C is one of the several invasive typhoidal *Salmonella enterica* serovars that cause enteric fever in humans, including *S.* Typhi (typhoid fever) and *S.* Paratyphi A, B, and C (paratyphoid fever). Still today, paratyphoid fever affects about five million people a year worldwide, resulting in 54,000 deaths (Crump and Mintz, 2010; World Health Organization, 2018). However, cases of *S.* Paratyphi C infection are not frequently reported, and the pathogen is no longer endemic in Europe (Achtman et al., 2012; Crump and Mintz, 2010; Liu et al., 2009; Uzzau et al., 2000). In contrast, *S.* Paratyphi C has been the only *Salmonella enterica* serovar found so far in specimens from medieval Europe (Zhou et al., 2018) and 16th-century Central America (a strain imported from Europe) (Vågene et al., 2018). Thus, *S.* Paratyphi C might have been the predominant typhoidal agent at the time.

Our phylogenetic reconstruction showed strong genomic stability of the *S.* Paratyphi C subgroup over at least one millennium. This is reflected in a small number of variants between the globally distributed ancient and modern genomes within the Paratyphi C clade, with the oldest genome dating to 1200 CE (Zhou et al., 2018) and the most recent to 2015 (Alikhan et al., 2018). Similarly, the three reconstructed genomes from Lübeck differed in only a few SNPs that were identified to have no effect on the phenotype (Table S5).

This aDNA study reports an epidemic outbreak of paratyphoid fever in Lübeck in the 14th century that killed at least 120 people. The infection dynamics were probably less pronounced and more localized than those of the previous plague. Nonetheless, the effects on life and trade must have been clearly felt. The consequences of the recurring disease outbreaks in the second half of the 14th century were severe and long lasting for Lübeck and the surrounding area, leading to collapsing bond and real estate markets, as well as increasing bankruptcy of local businesses. Moreover, the prospect of imminent death drove many citizens to make generous donations to churches and monasteries out of concern for the salvation of their souls (Fouquet and Zeilinger, 2011).

Limitations of the study

The main challenges in aDNA research are the small number of samples usually available for analysis and the poor DNA preservation. Due to a variety of environmental (Bollongino et al., 2008; Collins et al., 2002) and chemical (Warinner et al., 2017) factors, endogenous (human and pathogen) DNA is degraded over

time, rendering the recovery and analysis of any remaining DNA fragments often very difficult, if not impossible. In our study, we examined the skeletal remains of 92 individuals, a relatively large sample by aDNA standards. However, only 53 of them (~57.6%) contained sufficient human DNA for population genetic analyses. *S.* Paratyphi C DNA was even less abundant than human DNA in the extracts (Tables 1 and S3). In total, we identified *S.* Paratyphi C reads in eight individuals, and three of the generated data sets allowed for a full genome reconstruction. So far, only two other ancient *S.* Paratyphi C strains (Norway 1200 CE, Mexico 1545 CE) have been reported. Additional genomes from other historical periods and regions are therefore needed to provide a more comprehensive phylogeography of the pathogen.

Resource availability

Lead contact

Further information, requests, and inquiries should be directed to the lead contact, Ben Krause-Kyora (b.krause-kyora@ikmb.uni-kiel.de).

Materials availability

The study did not generate new unique reagents or materials.

Data and code availability

The accession number for the data reported in this paper is available through the European Nucleotide Archive: PRJEB41353 (https://www.ebi.ac.uk).

METHODS

All methods can be found in the accompanying Transparent methods supplemental file.

SUPPLEMENTAL INFORMATION

Supplemental information can be found online at https://doi.org/10.1016/j.isci.2021.102419.

ACKNOWLEDGMENTS

This study was supported by the Deutsche Forschungsgemeinschaft, Germany (DFG, German Research Foundation) through the projects 2901391021 (CRC 1266) and 390870439 (EXC 2150 – ROOTS) and the Medical Faculty of Kiel University, Germany. We thank Tal Dagan, Institute of General Microbiology, Kiel University, for her advice and helpful discussions.

AUTHOR CONTRIBUTIONS

A.N., S.H., and B.K.-K. conceived and designed the study. M.H., K.C., J.S., A.L.F., A.I., A.F., A.H., and A.K. generated and analyzed aDNA data. M.H., J.K., G.F., D.R., A.N., and B.K.-K. interpreted the results. M.H., A.N., B.K.-K. wrote and revised the manuscript with input from all the other authors.

DECLARATION OF INTERESTS

The authors declare no competing interests.

INCLUSION AND DIVERSITY

We worked to ensure diversity in experimental samples through the selection of the genomic data sets. The author list of this paper includes contributors from the location where the research was conducted who participated in the data collection, design, analysis, and/or interpretation of the work.

Received: December 21, 2020
Revised: February 22, 2021
Accepted: April 8, 2021
Published: May 21, 2021

REFERENCES

Achtman, M., Wain, J., Weill, F.X., Nair, S., Zhou, Z., and Sangal, V. (2012). Multilocus sequence typing as a replacement for serotyping in Salmonella enterica. PLoS Pathog. *8*, e1002776.

Alikhan, N.-F., Zhou, Z., Sergeant, M.J., and Achtman, M. (2018). A genomic overview of the population structure of Salmonella. PLoS Genet. *14*, e1007261.

Andrades Valtueña, A., Mittnik, A., Key, F.M., Haak, W., Allmäe, R., and Belinskij, A. (2017). The stone age plague and its persistence in Eurasia. Curr. Biol. *27*, 3683–3691.e8.

Benedictow, O.J. (2017). The Black Death, 1346–1353: The Complete History (Boydell Press).

Bhan, M.K., Bahl, R., and Bhatnagar, S. (2005). Typhoid and paratyphoid fever. Lancet *366*, 749–762.

Bollongino, R., Tresset, A., and Vigne, J.-D. (2008). Environment and excavation. Pre-lab impacts on ancient DNA analyses. Comptes. Rendus. Palevol. *7*, 91–98.

Bos, K.I., Schuenemann, V.J., Golding, G.B., Burbano, H.A., Waglechner, N., Coombes, B.K., McPhee, J.B., DeWitte, S.N., Meyer, M., Schmedes, S., et al. (2011). A draft genome of Yersinia pestis from victims of the Black Death. Nature *478*, 506–510.

Collins, M.J., Nielsen-Marsh, C.M., Hiller, J., Smith, C.I., Roberts, J.P., Prigodich, R.V., Wess, T.J., Csapò, J., Millard, A.R., and Turner-Walker, G. (2002). The survival of organic matter in bone: a review. Archaeometry *44*, 383–394.

Cooper, A., and Poinar, H. (2000). Ancient DNA. Do it right or not at all. Science *289*, 5482.

Crump, J.A., and Mintz, E.D. (2010). Global trends in typhoid and paratyphoid fever. Clin. Infect. Dis. *50*, 241–246.

Dollinger, P., and Krabusch, M. (1998). Die Hanse (Kröner).

Duggan, A.T., Perdomo, M.F., Piombino-Mascali, D., Marciniak, S., Poinar, D., Emery, M.V., Buchmann, J.P., Duchêne, S., Jankauskas, R., Humphreys, M., et al. (2016). 17th century Variola virus reveals the recent history of smallpox. Curr. Biol. *26*, 3407–3412.

Fouquet, G., and Zeilinger, G. (2011). Katastrophen im Spätmittelalter (Philipp von Zabern).

Grabowski, M., and Schmitt, G. (1993). Und das Wasser fließt in Röhren. Wasserversorgung und Wasserkünste in Lübeck. In Die Archäologie des Mittelalters und Bauforschung im Hanseraum, M. Gläser, ed. (Kulturhistorisches Museums Rostock), pp. 217–223.

Graßmann, A. (2005). Das Hansische Kontor zu Bergen und die Lübecker Bergenfahrer: International Workshop Lübeck 2003 (Schmidt-Römhild).

Haensch, S., Bianucci, R., Signoli, M., Rajerison, M., Schultz, M., Kacki, S., Vermunt, M., Weston, D.A., Hurst, D., Achtman, M., et al. (2010). Distinct clones of Yersinia pestis caused the black death. PLoS Pathog. *6*, e1001134.

Hammel-Kiesow, R. (2006). Häuser und Höfe in Lübeck. Historische, archäologische und baugeschichtliche Beiträge zur Geschichte der Hansestadt im Spätmittelalter und in der frühen Neuzeit (Wachholtz).

Hübler, R., Key, F.M., Warinner, C., Bos, K.I., Krause, J., and Herbig, A. (2019). HOPS: automated detection and authentication of pathogen DNA in archaeological remains. Genome Biol. *20*, 280.

Ibs, J.H. (1994). Die Pest in Schleswig-Holstein von 1350 bis 1547/48: Eine sozialgeschichtliche Studie über eine wiederkehrende Katastrophe. In Kieler Werkstücke: Reihe A, Beiträge zur schleswig-holsteinischen und skandinavischen Geschichte 12, E. Hoffmann, ed. (Peter Lang).

Kahlow, S. (2007). Die Pest als Interpretationsproblem mittelalterlicher und frühneuzeitlicher Massengräber. Bulletin der Schweizerischen Gesellschaft für Anthropologie *13*, 97–104.

Key, F.M., Posth, C., Esquivel-Gomez, L.R., Hübler, R., Spyrou, M.A., Neumann, G.U., Furtwängler, A., Sabin, S., Burri, M., Wissgott, A., et al. (2020). Emergence of human-adapted Salmonella enterica is linked to the Neolithization process. Nat. Ecol. Evol. *4*, 324–333.

Koppmann, K. (1884). In Die Chroniken der niedersächsischen Städte. Lübeck. Band 1 (S. Hirzel).

Koppmann, K. (1899). In Die Chroniken der niedersächsischen Städte. Lübeck. Band 2 (S. Hirzel).

Krause-Kyora, B., Nutsua, M., Boehme, L., Pierini, F., Pedersen, D.D., Kornell, S.-C., Drichel, D., Bonazzi, M., Möbus, L., Tarp, P., et al. (2018a). Ancient DNA study reveals HLA susceptibility locus for leprosy in medieval Europeans. Nat. Commun. *9*, 1569.

Krause-Kyora, B., Susat, J., Key, F.M., Kühnert, D., Bosse, E., Immel, A., Rinne, C., Kornell, S.-C., Yepes, D., Franzenburg, S., et al. (2018b). Neolithic and medieval virus genomes reveal complex evolution of hepatitis B. Elife *7*, e36666.

Liu, W.-Q., Feng, Y., Wang, Y., Zou, Q.-H., Chen, F., Guo, J.-T., Peng, Y.-H., Jin, Y., Li, Y.-G., Hu, S.-N., et al. (2009). Salmonella paratyphi C: genetic divergence from Salmonella choleraesuis and pathogenic convergence with Salmonella typhi. PLoS One *4*, e4510.

Lüdecke, T. (1980). Vom Brunnenwasser zum "Kunstwasser" – die Wasserversorgung im mittelalterlichen und frühneuzeitlichen Lübeck. In Archäologie in Lübeck. Erkenntnisse von Archäologie und Bauforschung zur Geschichte und Vorgeschichte der Hansestadt 3, K. Frerichs, ed. (Hansestadt Lübeck), pp. 97–100.

Lütgert, S.A. (2002). Archäologische Untersuchungen der Massenbestattungen am Heiligen-Geist-Hospital zu Lübeck: Auswertung der Befunde und Funde. In Lübecker Schriften zu Archäologie und Kulturgeschichte 26, M. Gläser, ed. (Rudolf Habelt), pp. 139–243.

O'Leary, N.A., Wright, M.W., Brister, J.R., Ciufo, S., Haddad, D., McVeigh, R., Rajput, B., Robbertse, B., Smith-White, B., Ako-Adjei, D., et al. (2016). Reference sequence (RefSeq) database at NCBI: current status, taxonomic expansion, and functional annotation. Nucleic Acids Res. *44*, D733–D745.

Prechel, M. (1996). Anthropologische Untersuchungen der Skelettreste aus einem Pestmassengrab am Heiligen-Geist-Hospital zu Lübeck. In Lübecker Schriften zu Archäologie und Kulturgeschichte 24, G.P. Fehring, ed. (Rudolf Habelt), pp. 323–339.

Prechel, M. (2002). Eine Lübecker Population von 1350 – Krankheiten und Mangelerscheinungen. In Lübecker Schriften zu Archäologie und Kulturgeschichte 26, M. Gläser, ed. (Rudolf Habelt), pp. 245–286.

Sánchez-Vargas, F.M., Abu-El-Haija, M.A., and Gómez-Duarte, O.G. (2011). Salmonella infections: an update on epidemiology, management, and prevention. Trav. Med. Infect. Dis. *9*, 263–277.

Schuenemann, V.J., Singh, P., Mendum, T.A., Krause-Kyora, B., Jäger, G., Bos, K.I., Herbig, A., Economou, C., Benjak, A., Busso, P., et al. (2013). Genome-wide comparison of medieval and modern Mycobacterium leprae. Science *341*, 179–183.

Schuenemann, V.J., Avanzi, C., Krause-Kyora, B., Seitz, A., Herbig, A., Inskip, S., Bonazzi, M., Reiter, E., Urban, C., Dangvard Pedersen, D., et al. (2018). Ancient genomes reveal a high diversity of Mycobacterium leprae in medieval Europe. PLoS Pathog. *14*, e1006997.

Singman, J.L. (1999). Daily Life in Medieval Europe (Greenwood Press).

Spyrou, M.A., Tukhbatova, R.I., Feldman, M., Drath, J., Kacki, S., Beltrán de Heredia, J., Arnold, S., Sitdikov, A.G., Castex, D., Wahl, J., et al. (2016). Historical Y. pestis genomes reveal the European black death as the source of ancient and modern plague pandemics. Cell Host Microbe *19*, 874–881.

Spyrou, M.A., Keller, M., Tukhbatova, R.I., Scheib, C.L., Nelson, E.A., Andrades Valtueña, A., Neumann, G.U., Walker, D., Alterauge, A., Carty, N., et al. (2019). Phylogeography of the second plague pandemic revealed through analysis of historical Yersinia pestis genomes. Nat. Commun. *10*, 4470.

Susat, J., Bonczarowska, J.H., Pētersone-Gordina, E., Immel, A., Nebel, A., Gerhards, G., and Krause-Kyora, B. (2020). Yersinia pestis strains from Latvia show depletion of the pla virulence gene at the end of the second plague pandemic. Sci. Rep. *10*, 14628.

Uzzau, S., Brown, D.J., Wallis, T., Rubino, S., Leori, G., and Bernard, S. (2000). Host adapted serotypes of Salmonella enterica. Epidemiol. Infect. *125*, 229–255.

Vågene, Å.J., Herbig, A., Campana, M.G., Robles García, N.M., Warinner, C., Sabin, S., Spyrou, M.A., Andrades Valtueña, A., Huson, D., Tuross, N., et al. (2018). Salmonella enterica genomes from victims of a major sixteenth-

century epidemic in Mexico. Nat. Ecol. Evol. *2*, 520–528.

Warinner, C., Herbig, A., Mann, A., Fellows Yates, J.A., Weiß, C.L., Burbano, H.A., Orlando, L., and Krause, J. (2017). A robust framework for microbial archaeology. Annu. Rev. Genomics Hum. Genet. *31*, 321–356.

World Health Organization. (2018). Typhoid Vaccines: WHO Position Paper – March 2018, Weekly Epidemiological Record No. 13, *93*, pp. 153–172. https://apps.who.int/iris/bitstream/handle/10665/272272/WER9313.pdf.

Yue, R.P.H., Lee, H.F., and Wu, C.Y.H. (2017). Trade routes and plague transmission in pre-industrial Europe. Sci. Rep. *7*, 12973.

Zhou, Z., Lundstrøm, I., Tran-Dien, A., Duchêne, S., Alikhan, N.-F., Sergeant, M.J., Langridge, G., Fotakis, A.K., Nair, S., Stenøien, H.K., et al. (2018). Pan-genome analysis of ancient and modern Salmonella enterica demonstrates genomic stability of the invasive para C lineage for millennia. Curr. Biol. *28*, 2420–2428.e10.

Zhou, Z., Alikhan, N.-F., Mohamed, K., Fan, Y., and Achtman, M. (2020). The EnteroBase user's guide, with case studies on Salmonella transmissions, Yersinia pestis phylogeny, and Escherichia core genomic diversity. Genome Res. *30*, 138–152.

iScience, Volume *24*

Supplemental information

Mass burial genomics reveals outbreak of enteric paratyphoid fever in the Late Medieval trade city Lübeck

Magdalena Haller, Kimberly Callan, Julian Susat, Anna Lena Flux, Alexander Immel, Andre Franke, Alexander Herbig, Johannes Krause, Anne Kupczok, Gerhard Fouquet, Susanne Hummel, Dirk Rieger, Almut Nebel, and Ben Krause-Kyora

SUPPLEMENTARY FIGURES

HGH-924

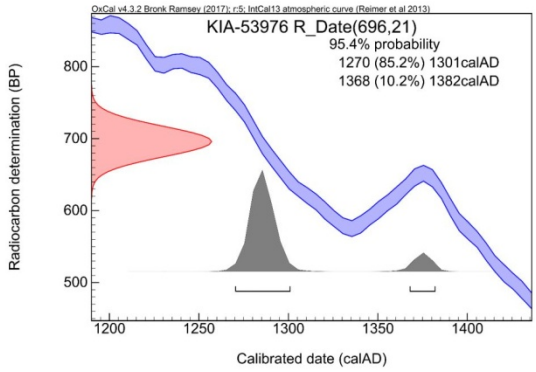

HGH-950

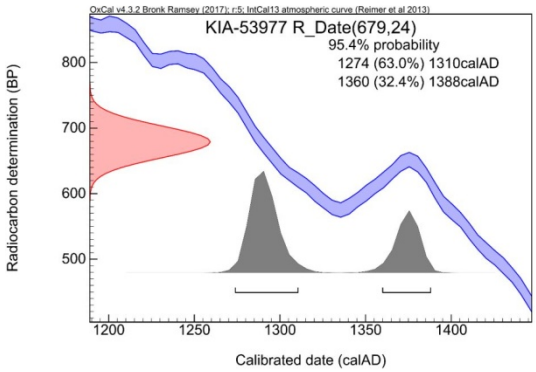

HGH-1429

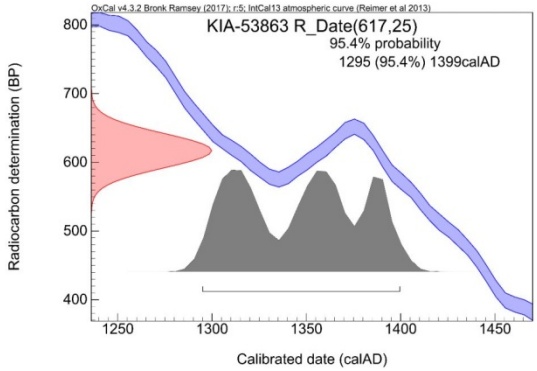

HGH-1579

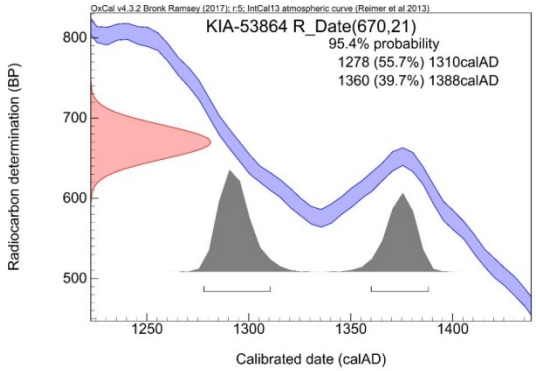

HGH-1600

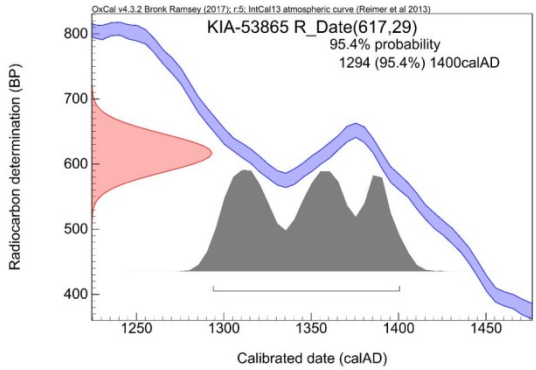

Figure S1. Radiocarbon dates on bone collagen. Atmospheric curves and radiocarbon date determination of the samples HGH-924, HGH-950, HGH-1429, HGH-1579 and HGH-1600. The analyses were performed by the Leibniz Laboratory for Radiometric Dating and Stable Isotope Research at Kiel University. (Related to Figure 1 and Table 1 of main text and Table S1).

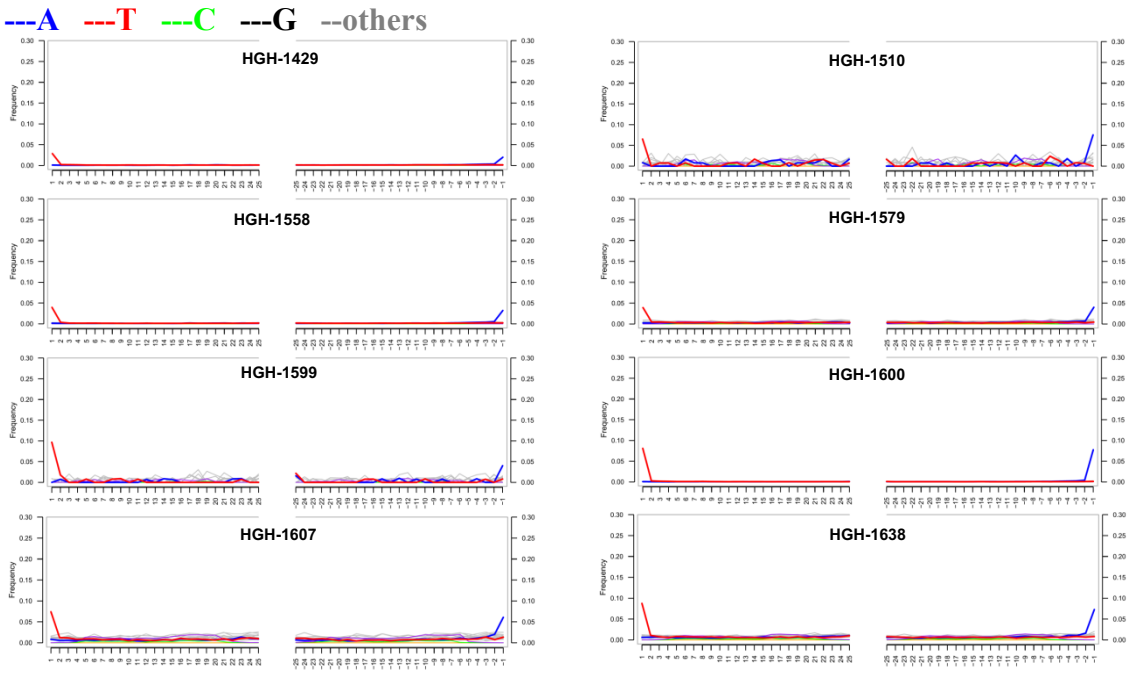

Figure S2. *S.* Paratyphi C aDNA damage patterns. Damage plots of the eight HGH samples with reads mapping to *Salmonella enterica* in the metagenomic analysis. Plots were generated with mapDamage after alignment to the *S.* Paratyphi C RKS4594 (NC_012125.1) reference genome. (Related to Table 1 of main text).

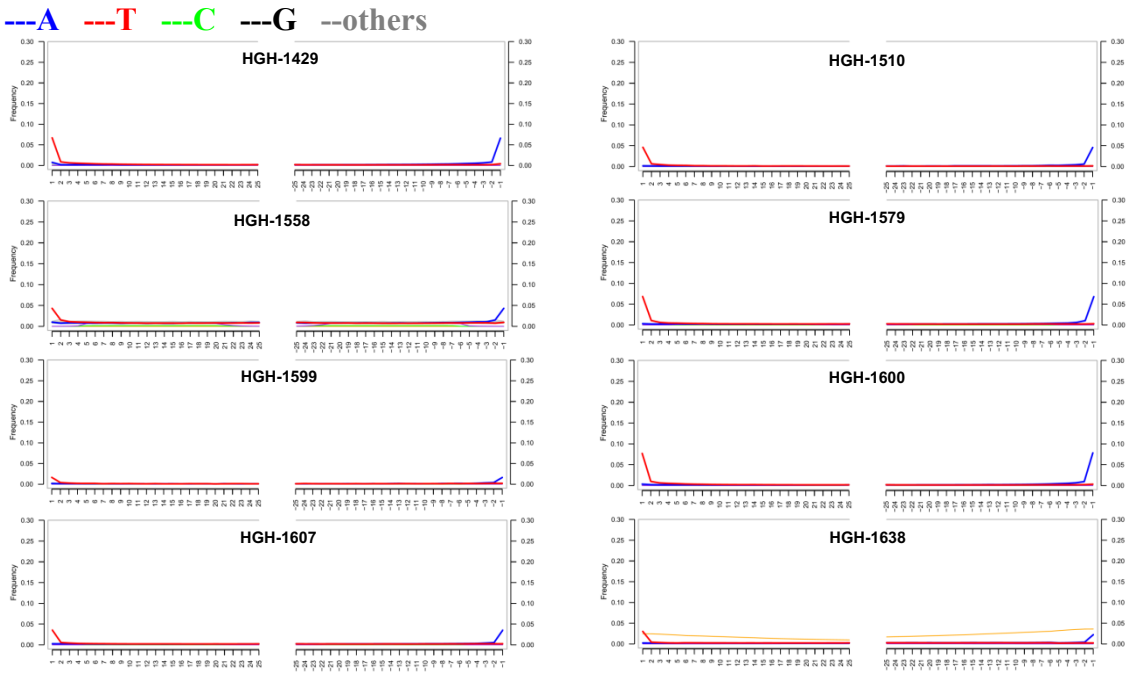

Figure S3. Human aDNA damage patterns. Damage plots of the eight HGH samples with reads mapping to *Salmonella enterica* in the metagenomic analysis. Plots were generated with mapDamage after alignment to the *Homo sapiens* hg19 reference genome. (Related to Table 1 of main text).

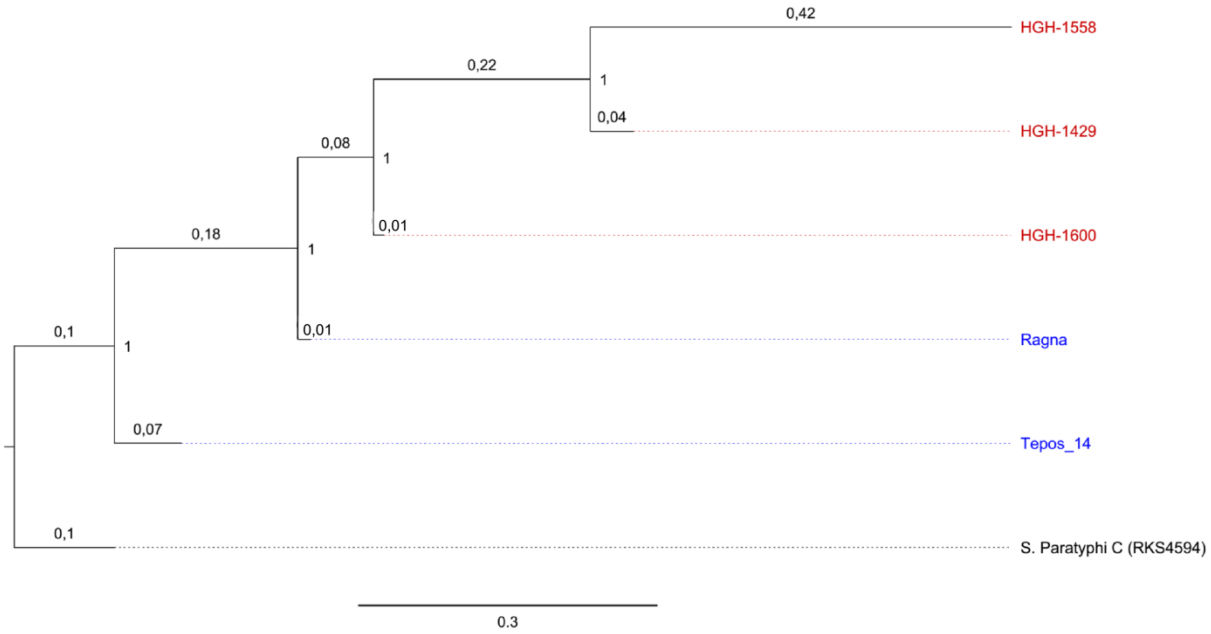

Figure S4. Phylogenetic relationship of ancient and modern *S.* Paratyphi C genomes. Bayesian phylogenetic tree of three genomes from the HGH mass burial in Lübeck (red), the ancient *S.* Paratyphi C strains Ragna (Norway 1200 CE) and Tepos_14 (Mexico 1545 CE) (blue) and the reference genome of modern *S.* Paratyphi C (RKS4594) (black). The tree is based on a minimal SNP coverage of 5x and 236,622 variant positions. Nodes are labeled with the posterior probability value assigned by MrBayes. Branch lengths correspond to number of substitutions per site. (Related to Figure 2 of main text and Table S5).

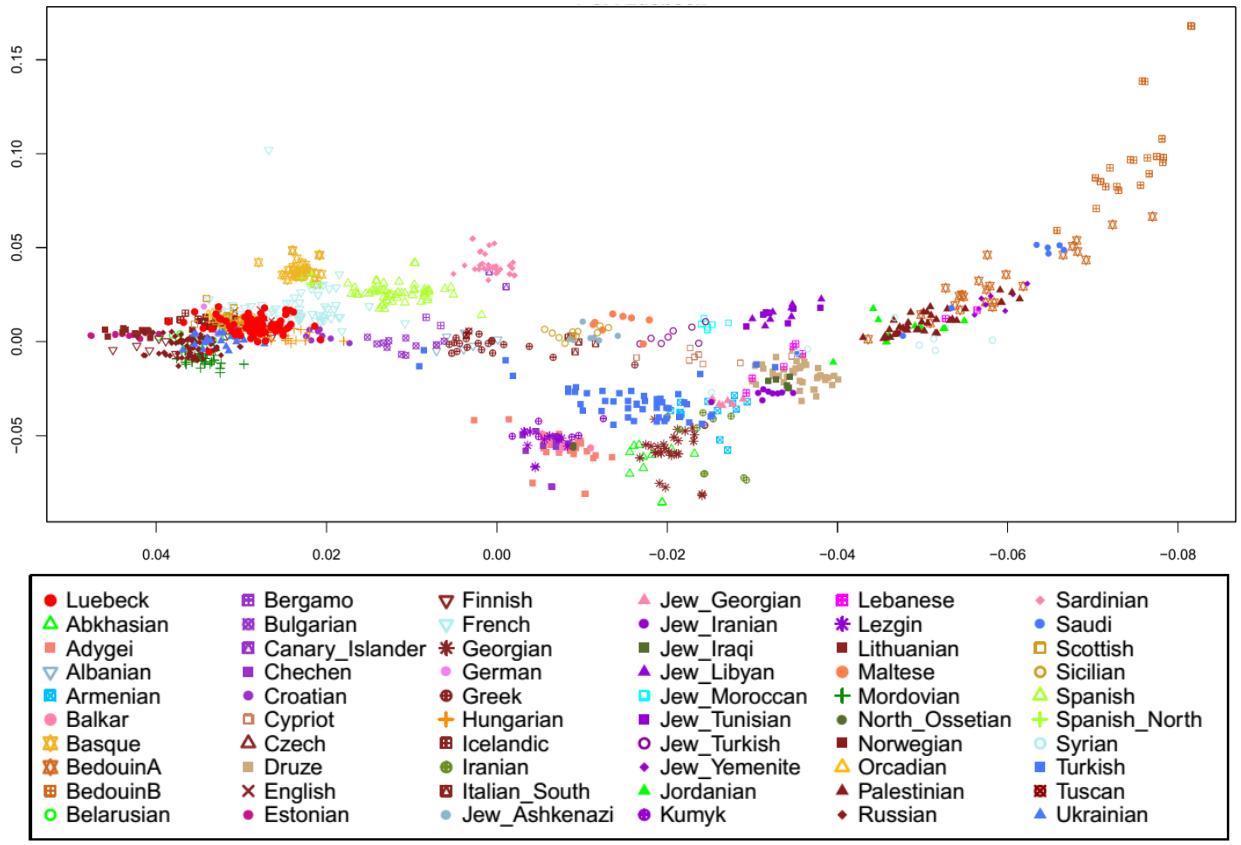

Figure S5. Population genetic analysis. Principal component analysis (PCA) of HGH individuals (red circles) from Lübeck in the context of 59 modern-day West-Eurasian populations. A PCA with a smaller set of reference populations is shown in Figure 3. (Related to Figure 3 of main text and Figure S6).

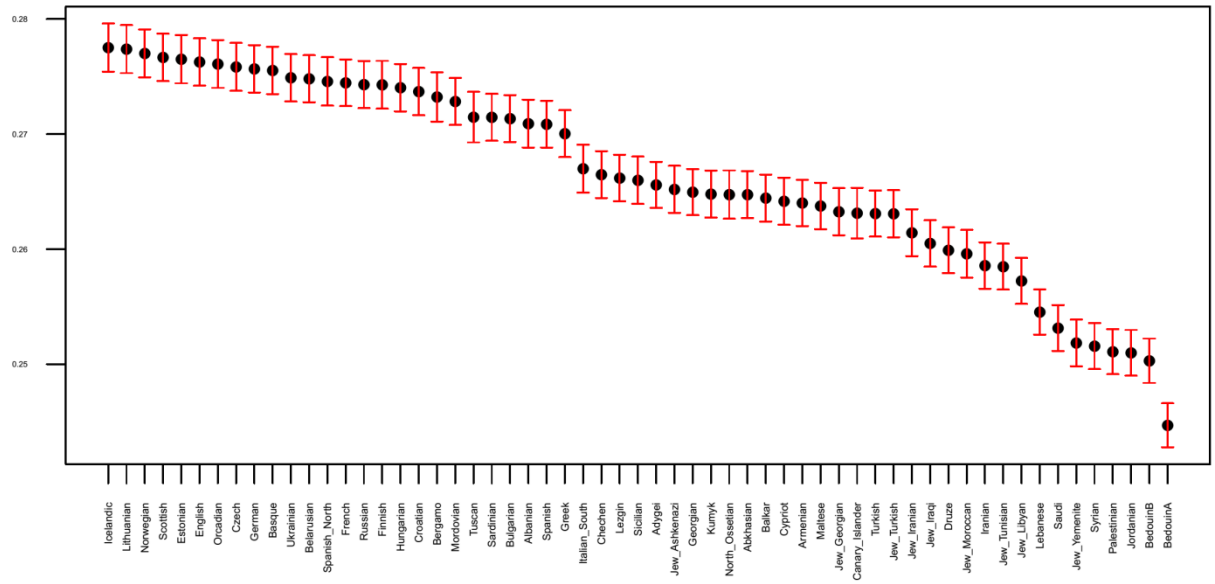

Figure S6. Population genetic analysis. F3-statistics of HGH individuals from Lübeck in the context of 59 modern-day West-Eurasian populations. Genetic distances were calculated with respect to the HGH population. F3-statistics reveal affinities between HGH individuals and those from northern Britain, eastern Europe and the Balkans. (Related to Figure 3 of main text and Figure S5).

SUPPLEMENTARY TABLES

Table S1. Radiocarbon dates on bone collagen. The analyses were performed by the Leibniz Laboratory for Radiometric Dating and Stable Isotope Research at Kiel University. (Related to Figure 1 and Table 1 of main text and Figure S1).

Sample	Context	pMC[a]	Age (BP)	$\delta^{13}C$ (‰)
HGH-942	4528	91.71 ± 0.24	696 ± 21	-20.2 ± 0.1
HGH-950	4528	91.90 ± 0.27	679 ± 24	-21.1 ± 0.2
HGH-1429	4571	92.61 ± 0.28	617 ± 25	-19.9 ± 0.1
HGH-1579	4571	92.00 ± 0.24	670 ± 21	-19.2 ± 0.2
HGH-1600	4571	92.61 ± 0.33	617 ± 29	-20.0 ± 0.1

[a]pMC denotes the percentage of modern carbon, based on the hypothetical value of the atmosphere in 1950, corrected to $\delta^{13}C$ = -25 ‰ using the $\delta^{13}C$ value determined by AMS

Table S2. STR typing results. Genetic fingerprinting for HGH samples from Lübeck included in this study. (Related to Table 1 of main text).

				Genetic fingerprinting						
ID	Context	Sex[a]	Age[a]	Amelogenin	D13S317	D21S11	D18S51	TH01	D5S818	FGA
886	4528	F	26-32	-/-	-/-	-/-	-/-	-/-	10/-	-/-
888	4528	F	40-60	-/-	-/-	-/-	-/-	-/-	-/-	-/-
892	4528	M	40-50	-/-	-/-	-/-	-/-	-/-	-/-	-/-
894	4528	M	40+	-/-	-/-	-/-	-/-	-/-	-/-	-/-
909	4528	M	30-50	-/-	-/-	-/-	-/-	7/-	-/-	-/-
924	4528	M	23-35	-/-	-/-	-/-	-/-	-/-	-/-	-/-
926	4528	M[b]	18-21	X/-	12/-	28/-	-/-	9/9.3	12/-	-/-
927	4528	M	20-23	-/-	-/-	-/-	-/-	-/-	-/-	22.2/-
930	4528	M	18-23	-/-	-/-	-/-	-/-	-/-	-/-	-/-
934	4528	F	25-35	X/X	12/-	27/29	13/20	6/9.3	12/-	20/22
942	4528	F	28-32	X/X	12/-	30/31.2	15/16	6/9	11/12	21/24
943	4528	M[c]	37-41	X/X	8/12	30/32.2	13/16	(8/9/10)	12/-	20/22
947	4528	M	23-40	-/-	-/-	-/-	-/-	-/-	-/-	-/-
948	4528	M	40-46	Y/-	-/-	-/-	-/-	6/-	-/-	22/-
950	4528	M	40-55	X/Y	11/12	30.2/32	17/-	6/8	12/-	21/22
1006	4528	M	30-36	X/Y	12/-	28/30.2	12/18	6/-	11/13	21/21.2
1219	4528	M	21-25	(X)/Y	9/11	29/-	13/-	6/8	12/-	-/-

1226	4528	M	35-45	X/Y	11/12	(29)/(30)/31/31.2	17/-	8/9	11/13	22/-
1227	4528	M	32-37	X/Y	12/-	30/(31.2)/(32.2)	13/14	7/9.3	11/12	24/25
1415	4528	M	23-40	X/Y	8/11	29/30	12/19	6/9.3	8/9	17/20
1440	4528	M	62-75	X/Y	9/11	29/30	12/15	9.3/-	12/14	21/24
1441	4528	M	67-75	X/Y	8/12	30/-	12/15	9.3/-	13/-	22/25
1449	4528	M	24-30	X/Y	11/12	(32.2)/33.2	-/-	9/9.3	11/-	25/26
1476	4528	M	36-45	X/Y	12/-	29/31.2	12/-	7/9.3	11/12	20/23
1551	4528	M	44-49	X/Y	10/11	28/29	18/19	7/-	11/12	20/22
1699	4528	M	40-45	X/Y	11/12	28/-	12/16	7/9.3	9/11	24/-
1701	4528	F[c]	20-26	X/Y	12/13	31.2/-	15/18	9/9.3	11/-	23/23.2
1702	4528	M	20-23	X/Y	10/12	30/-	12/-	7/8	12/13	(21/23/24)
1710	4528	M	55-60	X/Y	9/12	28/((31.2))/32.2	13/15	7/9	11/12	21/23
1133	4529	M	28-34	X/Y	12/14	29/((32.2))/33.2	12/17	7/9.3	10/12	22/24
1154	4529	M	32-36	X/Y	8/12	30.2/31	15/16	6/-	13/-	21/23
1156	4529	M	21-24	X/Y	12/-	29/30	15/-	8/-	12/13	-/-
1172	4529	M	49-53	X/Y	12/14	28/31	14/16/(19)	7/9.3	(10/12/13)	21/24
1234	4529	M	20-26	X/Y	8/14	27/29	14/15	7/9.3	11/12	19/22
1571	4529	M	20-26	Y/-	11/-	-/-	12/15	7/9.3	11/12	18/22
1612	4529	M	20-26	X/Y	11/13	28/-	13/15	7/9.3	10/12	20/23
1627	4529	M	63-68	X/Y	11/-	29/30	11/19	7/9.3	11/12	25/-
1664	4529	M	59-70	X/Y	10/11	28/-	16/-	9/9.3	11/13	21/25
1730	4529	M	29-35	X/Y	12/-	-/-	15/20	6/9	12/-	-/-
1780	4529	M	24-29	X/Y	11/12	28/-	13/14	9.3/-	11/12	21/24
1483	4562	M	25-30	X/Y	11/-	29/30	12/17	9.3/-	11/12	21/22
1525	4562	F	60-70	X/X	8/10	29/31.2	12/(13)	9/9.3	11/-	22/-
1526	4562	M	30-50	X/Y	11/12	30/33.2	14/-	7/8	12/13	23/25
1575	4562	F	49-54	X/X	8/11	29/-	16/17	9.3/-	11/12	21/24
1577	4562	M	65-80	X/Y	9/12	28/((31.2))/32.2	15/16	6/9.3	11/12	20/25
1578	4562	M[c]	49-54	X/X	11/12	29/30	12/17	8/9	9/11	22.2/24
1579	4562	M[c]	18-23	X/X	11/14	28/30	12/-	6/7	11/13	22/-
1580	4562	M	32-50	X/Y	12/13	31/(32)	(13)/16/18	9/9.3	11/12	19/20
1607	4562	M	64-75	X/Y	12/13	32.2/-	14/16	9.3/-	12/-	21/22
1608	4562	F	19-24	X/X	10/12	29/((30.2))/31.2	14/15	9.3/-	9/11	24/-
1628	4562	F	63-70	X/X	12/13	30/((31.2))/(((32))/33.2	12/16	7/9.3	8/9	22/-
1633	4562	F	57-62	X/X	13/14	30/33.2	16/18	6/9.3	12/-	19/20
1662	4562	M	36-40	-/-	-/-	-/-	-/-	-/-	-/-	-/-
1286	4571	F	21-24	X/X	8/-	28/29	17/19	8/9.3	12/-	21/22

1316	4571	M	33-38	X/Y	11/15	29/30.2	17/19	9.3/-	11/-	22/-
1319	4571	F	67-75	X/X	12/-	29/32.2	13/17	7/9.3	11/12	19/25
1391	4571	F	45-50	X/X	12/-	(28)/(29)/30	12/18	9/9.3	11/12	20/21
1392	4571	M	22-25	X/Y	11/12	28/31.2	16/-	8/-	11/12	19/22
1408	4571	F	67-75	X/X	12/-	31/-	14/-	6/8	12/-	23/25
1409	4571	F[c]	23-26	X/Y	12/-	30/32.2	13	7/9.3	9/12	21/22
1410	4571	F	55-60	X/X	10/11	30/-	14/17	6/9.3	12/-	24/-
1426	4571	F	62-70	-/-	10/-	-/-	14/-	9.3/-	-/-	22/-
1427	4571	M[c]	45-52	X/X	11/12	28/29	13/16	6/7	11/-	21/24
1429	4571	M	22-25	X/Y	10/11	-/-	13/15	6/9.3	10/11	20/-
1455	4571	F	18-23	-/-	-/-	-/-	-/-	-/-	-/-	-/-
1458	4571	F	60-80	X/X	12/-	28/32	15/17	8/9.3	(10)/12	20/22
1459	4571	M[b]	18-23	X/-	12/-	29/32.2	18/-	8/9	11/12	21/-
1467	4571	M	47-63	X/Y	10/11	28/((29))/30	14/-	6/7	11/12	22/25
1499	4571	M	23-40	X/Y	11/13	29/31.2	13/16	8/-	11/13	18/20
1508	4571	F	19-26	-/-	-/-	-/-	-/-	-/-	-/-	-/-
1510	4571	F	60-66	X/-	8/11	28/31.2	12/14	7/-	12/-	-/-
1511	4571	F	64-75	X/X	9/10	27/((28))/((29))/30	12/15	6/9.3	9/12	23/24
1512	4571	F	30-48	X/X	11/15	28/((29))/30	15/17	9/9.3	9/12	22/-
1516	4571	M	30-60	X/Y	8/12	29/((33.2))/34.2	12/14	8/9.3	11/13	20/21
1517	4571	M[b]	40-60	X/-	-/-	31.2/-	13/15	9/-	11/-	19/20
1518	4571	M[b]	20-26	X/-	11/12	32/-	12/-	7/9	11/-	20/-
1556	4571	F	23-30	X/X	8/12	32.2/-	13/15	9.3/-	12/13	25/26
1557	4571	M[b]	51-56	X/-	-/-	30/-	17/-	8/-	-/-	24/-
1558	4571	M	66-75	X/Y	(9/10/11)	-/-	(14/18/19)	6/9	11/-	-/-
1559	4571	F	20-30	X/X	9/12	31.2/32.2	13/15	6/9.3	11/13	18/21
1599	4571	F	42-48	X/X	9/11	27/((32.2))/33.2	11/16	8/9	13/-	22/25
1600	4571	M	40-45	X/Y	11/14	29/30.2	14/-	9/9.3	11/12	18/24
1601	4571	M	53-58	X/Y	11/13	28/29	14/17	6/9.3	10/15	21/24
1602	4571	F	18-23	X/X	11/14	28/29	13/-	7/-	11/-	21/-
1617	4571	M[b]	52-66	X/-	12/14	29/-	15/17	6/9	12/-	20/23
1635	4571	M	52-57	X/Y	8/10	31/32.2	14/16	6/9	11/12	20/22
1636	4571	F[c]	52-57	X/Y	11/13	29/((30))/((31))/32	14/15	6/9.3	12/14	19/22
1637	4571	M	49-55	X/Y	12/-	29/((31.2))/32.2	-/-	9.3/-	10/11	21/-
1638	4571	F	53-58	X/X	11/12	29/34.2	14/21	8/9	11/12	21/23
1639	4571	F	40-80	X/X	8/10	30/32.2	13/15	9/9.3	11/13	22/25
1653	4571	M	47-52	X/Y	9/(11)/14	29/((30))/((30.2))/31.2	(14)/17/18	8/9	12/-	20/21

1655	4571	M	29-54	X/Y	11/12	27/((28))/((29))/30	14/16	7/8	9/12	20/23

[a] Refers to the results of the osteological analysis

- Only one allele detected due to homozygosity or allelic dropout

M[b] Morphologically and genetically determined sex differs. The genetically determined sex may be due to a dropout of the Y-chromosomal allele (incomplete STR typing).

F[c]/M[c] Morphologically and genetically determined sex differs. Due to a complete STR typing the genetically determined sex should be given priority.

(()) Most likely overamplified stutter artifacts. Specifically, for the locus D21S11 this type of artifact is well known from self-designed and commercially available multiplex kits.

() Additional allele(s) occur(s). These alleles may be the result of overamplified artifacts or a drop-in event. It remains uncertain which alleles are authentic.

Table S3. Summary Table. Complete list of HGH samples included in this study. (Related to Figure 3 and Table 1 of main text).

Sample ID[a]	Context[a]	Sex[b]	Age[b]	Skeletal elem.[c]	#Reads total (C&M)[d]	# Reads *S. enterica*[e]	# Reads *S.* Paratyphi C[f]	Score[g]	# Ancient reads[h]	HG[i]	PCA[j]	Endogenous DNA (%)[k]
886	4528	F	26-32	Femur	13,625,657	7						0.1
888	4528	F	40-60	Femur	10,194,752	10			1			0.1
892	4528	M	40-50	Femur	11,862,622	25						0.2
894	4528	M	40+	Meta tarsus	54,740,829	16						0.1
909	4528	M	30-50	Tooth	19,447,917	9						0.1
924[m]	4528	M	23-35	Tooth	4,656,827	0						0.8
926	4528	M[1]	18-21	Tooth	25,158,177	26			1			0.2
927	4528	M	20-23	Tooth	23,646,240	22						0.1
930	4528	M	18-23	Femur	22,125,625	18			2			0.2
934	4528	F	25-35	Tooth	9,827,192	0				H1	X	26.9
942	4528	F	28-32	Tooth	6,773,853	0				R0	X	12.4
943	4528	M[2]	37-41	Tooth	18,242,433	0				H1	X	16.7
947	4528	M	23-40	Petrous bone	5,734,946	0						0.4
948	4528	M	40-46	Tooth	9,582,406	14			1			0.1
950[m]	4528	M	40-55	Tooth	18,119,081	10				H2	X	24.4
1006	4528	M	30-36	Tooth	7,920,752	7			2		X	47.1
1219	4528	M	21-25	Tooth	9,883,962	24			3	U4		2.3
1226	4528	M	35-45	Tooth	8,780,302	5				K1	X	30.8
1227	4528	M	32-37	Tooth	5,095,480	2				H1	X	54.8
1415	4528	M	23-40	Tooth	10,425,777	15			1	H1	X	30.4
1440	4528	M	62-75	Tooth	7,608,778	16			2		X	11.5

1441	4528	M	67-75	Tooth	8,484,255	23			3		X	15.9
1449	4528	M	24-30	Tooth	7,411,379	40			2			1.7
1476	4528	M	36-45	Tooth	9,218,640	4					X	13.6
1551	4528	M	44-49	Tooth	6,312,828	11			1			3.8
1699	4528	M	40-45	Tooth	6,270,615	352	682	-0.041		HV	X	36.5
1701	4528	F[2]	20-26	Tooth	4,898,711	41				JT		5.0
1702	4528	M	20-23	Tooth	6,286,548	44						5.6
1710	4528	M	55-60	Tooth	6,581,118	43						12.8
1133	4529	M	28-34	Tooth	10,077,065	10			2		X	22.0
1154	4529	M	32-36	Tooth	4,842,018	2			1	I	X	48.8
1156	4529	M	21-24	Tooth	6,552,887	24			7			2.0
1172	4529	M	49-53	Tooth	7,980,774	4			1	J1	X	38.1
1234	4529	M	20-26	Tooth	10,714,325	9			1	T2	X	66.3
1571	4529	M	20-26	Tooth	10,276,425	20			3			1.3
1612	4529	M	20-26	Tooth	5,785,789	33				HV		14.6
1627	4529	M	63-68	Tooth	6,131,199	43						1.5
1664	4529	M	59-70	Tooth	6,283,524	30					X	23.2
1730	4529	M	29-35	Tooth	7,100,372	36				H1	X	30.6
1780	4529	M	24-29	Tooth	6,032,043	35				H1		59.3
1483	4562	M	25-30	Tooth	296,206	1						11.8
1525	4562	F	60-70	Tooth	5,042,620	2				K1	X	44.3
1526	4562	M	30-50	Tooth	16,374,285	8				H1	X	6.4
1575	4562	F	49-54	Tooth	10,312,193	3					X	26.5
1577	4562	M	65-80	Tooth	14,583,068	15				U5	X	62.0
1578	4562	M[2]	49-54	Tooth	8,591,236	3				H6	X	19.7
1579[l,m]	4562	M[2]	18-23	Tooth	419,943,997	156,323	32,287	0.007	51			0.5
1580	4562	M	32-50	Tooth	10,803,343	10				U8	X	26.2
1607[l]	4562	M	64-75	Tooth	128,490,993	7,500	8,354	0.003	315	H2	X	20.4
1608	4562	F	19-24	Tooth	10,442,770	1				U2	X	0.222
1628	4562	F	63-70	Tooth	14,202,741	2					X	0.523
1633	4562	F	57-62	Tooth	14,511,703	9				H5	X	15.7
1662	4562	M	36-40	Tooth	12,632,005	27			3	X		2.3
1286	4571	F	21-24	Tooth	2,725,423	8						2.6
1316	4571	M	33-38	Tooth	10,883,827	37			2	T1	X	8.7
1319	4571	F	67-75	Tooth	6,127,663	37			2	U8	X	29.9
1391	4571	F	45-50	Tooth	3,777,477	3				H1	X	20.6
1392	4571	M	22-25	Tooth	14,584,536	95			1	K1		2.2
1408	4571	F	67-75	Tooth	7,787,795	18						3.3

1409	4571	F[2]	23-26	Tooth	18,366,406	24			1		X	4.5
1410	4571	F	55-60	Tooth	8,167,491	10				H1	X	14.2
1426	4571	F	62-70	Femur	7,088,473	0						0.8
1427	4571	M[2]	45-52	Tooth	2,428,582	0				R1		19.0
1429[l,m]	4571	M	22-25	Tooth	451,266,651	504,232	155,502	0.039	275	J1	X	1.2
1455	4571	F	18-23	Humerus	10,638,683	19						0.1
1458	4571	F	60-80	Tooth	537,979,602	197,213	12,241	-0.022	79	U5	X	1.2
1459	4571	M[1]	18-23	Tooth	5,881,509	4						5.0
1467	4571	M	47-63	Tooth	13,521,186	0				R0	X	5.1
1499	4571	M	23-40	Tooth	3,606,575	1				H1	X	27.2
1508	4571	F	19-26	Femur	6,367,115	8				W5		0.2
1510[l]	4571	F	60-66	Tooth	15,763,343	407	675	0.001	13		X	10.6
1511	4571	F	64-75	Tooth	16,592,652	11					X	41.0
1512	4571	F	30-48	Tooth	7,378,133	0				X2	X	53.2
1516	4571	M	30-60	Tooth	4,454,874	27			1	T2	X	16.8
1517	4571	M[1]	40-60	Tooth	15,965,894	5					X	6.4
1518	4571	M[1]	20-26	Tooth	14,591,977	7						1.7
1556	4571	F	23-30	Tooth	9,469,187	6				J1	X	61.0
1557	4571	M[1]	51-56	Femur	13,573,557	7			1	H1		2.5
1558[l]	4571	M	66-75	Tooth	430,839,256	198,088	113,324	0.029	343	K1	X	0.8
1559	4571	F	20-30	Tooth	10,911,613	2				U5	X	53.9
1599[l]	4571	F	42-48	Tooth	6,435,352	464	442	0.011	14		X	11.3
1600[l,m]	4571	M	40-45	Tooth	339,436,728	641,231	135,367	0.067	668	H2	X	58.8
1601	4571	M	53-58	Tooth	13,385,552	13			1	R		3.5
1602	4571	F	18-23	Tooth	7,352,266	3				H1		4.1
1617	4571	M[1]	52-66	Tooth	9,222,778	0						5.2
1635	4571	M	52-57	Tooth	13,479,959	2				H1	X	32.4
1636	4571	F[2]	52-57	Tooth	10,010,869	3					X	30.6
1637	4571	M	49-55	Tooth	12,199,289	118	685	-0.002	5	R0		1.8
1638[l]	4571	F	53-58	Tooth	133,292,730	10,034	5,946	0.003	510	J1	X	13.4
1639	4571	F	40-80	Tooth	16,468,848	1				X2	X	61.0
1653	4571	M	47-52	Tooth	12,670,312	25			1			2.7
1655	4571	M	29-54	Tooth	16,932,750	1				W3	X	4.9

[a]Corresponds to the archaeological find and context number; [b]Sex and Age refer to the results of the osteological analysis; [c]Skeletal element defines the sample type from which DNA was extracted; [d]Total number of reads after clipping and merging; [e]Number of reads assigned to the taxonomic node of *S. enterica* subsp. *enterica* in the metagenomic analysis by MALT; [f]Number of reads aligned to the reference of *S.* Paratyphi C RKS4594 (NC_012125) in the multi-reference serovar determination; [g]Taxa-specific mapping score for *S.* Paratyphi C (see Transparent Methods); [h]Number of authentic ancient reads identified by MaltExtract; [i]Mitochondrial haplogroups

determined by HaploFind; [j]Samples included in the population genetic analyses (Figure 3 and Figures S5 - S6); [k]Given as proportion of reads mapped to the human genome relative to the total reads (%); [l]Samples found to be *S.* Paratyphi C-positive (Table 1); [m]Samples used for radiocarbon dating (Figure S1 and Table S1).

Table S4. Multi-reference mapping. List of *Salmonella enterica* reference genomes used in the multi-reference mapping. (Related to Table 1 of main text).

***S. enterica* serovar**	**Strain**	**NCBI Accession Number**
Bareilly	CFSAN000191	CP032622.1
Choleraesuis	SC-B67	NC_006905.1
Dublin	USMARC-69838	CP032449.1
Enteritidis	ATCC BAA-708	CP025554.1
Gaminara	CFSAN070644	CP024165.1
Heidelberg	5	CP031359.1
Inverness	ATCC 10720	CP019181.1
Johannesburg	ST203	CP019411.1
Kentucky	PU131	CP026327.1
Paratyphi A	AKU_12601	FM200053.1
Paratyphi B	SPB7	CP000886.1
Paratyphi C	RKS4594	NC_012125.1
Typhi	CT18	NC_003198.1
Typhimurium	14028S	CP001363.1
Weltevreden	1655	CP014996.1

Table S5. Variant call statistics. Matrix showing the single-nucleotide polymorphism (SNP) calls among the ancient *S.* Paratyphi C genomes from Lübeck, Ragna and Tepos_14 relative to the reference genome of Paratyphi C RKS4594, with a minimal coverage of 5x per call. (Related to Figure 2 of main text and Figure S4).

Strain	***S.* Paratyphi C RKS4594**	**1429**	**1558**	**1600**	**Ragna**	**Tepos_14**
1429	461	-	4	2	54	194
1558	314		-	2	50	135
1600	806			-	112	403
Ragna	858				-	526
Tepos_14	625					-

TRANSPARENT METHODS

Archaeological background

The human remains analysed in this study were recovered during archaeological excavations next to the Heiligen-Geist-Hospital in Lübeck in the early 1990s (Lütgert, 2002). The archaeological context consisted of two mass graves (4528 and 4529, *n=696*) and two smaller burial pits (4562 and 4571, *n=120*). According to the archaeological documentation, the pits 4562 and 4571 cut into the contexts 4528 and 4529 and are therefore dated younger (Prechel, 2002). Osteological age and sex as well as genetic sex are listed in Tables S2 and S3, respectively.

Precautions

Extraction and all pre-PCR steps were carried out in two dedicated aDNA clean rooms (at Kiel University and Göttingen University) following the guidelines on contamination control for aDNA studies (Cooper and Poinar, 2000), including cleaning of surfaces and re-usable tools with bleach or ready-to-use solutions for removing nucleic acid contaminants and UV radiation before and after use. The commercially certified DNA/RNA-free consumables were additionally irradiated with UV light before use. Negative controls were taken along during the extraction (one control for every 22 samples, without bone/tooth powder) and the library preparation (an additional control for every 22 samples, using ddH_2O instead of aDNA extract). Wearing of protective clothing, including disposable coveralls, masks and two layers of gloves were mandatory. As a further means of authentication, STR profiles at seven loci were generated. Pre- and post PCR amplification steps were carried out in separate laboratories, located in independent buildings. Furthermore, no studies on ancient or modern *S. enterica* material have been conducted in any of our laboratory facilities before this analysis.

DNA extraction

For the study, teeth and/or bones from 92 individuals (4528, *n=29*; 4529, *n=11*; 4562, *n=13*; 4571, *n=39*) were sampled. DNA extracts were generated at the Department of Historical Anthropology and Human Ecology at the University of Göttingen using a protocol modified from Fehren-Schmitz et al. (2010). To remove possible cellular contamination from the sample surfaces, the tooth roots were exposed to a 6% sodium hypochlorite solution (Aug. Hedinger GmbH & Co. KG, Stuttgart, Germany) and rinsed afterwards with purified water (Barta et al., 2013; Kemp and Smith, 2005). For the bone samples, the outer surface was mechanically removed using an electric drill with a diamond tipped saw blade (K10, KaVo, Germany).

Subsequently, the samples were mechanically pulverized in a ball triturator (MM200, Retsch). For decalcification and lysis, 200 mg pulverized sample material was incubated in 1000 µL EDTA (0.5 M, pH 8.0, Invitrogen™) and 50 µL proteinase K solution in Tris/HCl (pH 7.5, 0.01 mol/L, 600 mAnson-U/mL, Merck) for 18 h at 37 °C under constant inversion. In a second lysis step, another 50 µL proteinase K solution was added to the sample and incubated for further 2 h at 56 °C. 20 µL sodium dodecyl sulphate (10 mg/mL, Sigma-Aldrich®) were added and incubated for 5 min at 65 °C. The lysate was centrifuged for 3 min at 3300 rcf. 1000 µL of the supernatant of each sample was subjected to an automated DNA extraction (BioRobot® EZ1 Advanced, Qiagen) by using a custom-made version of the Large-Volume-Protocol (Qiagen) and the EZ1 DNA Investigator® Kit (Qiagen) following the manufacturer's instructions. The DNA was eluted in 100 µL TE Buffer. The DNA extracts were stored at -22 °C. In addition, DNA extractions from six teeth were performed at the Institute of Clinical Molecular Biology (IKMB) in Kiel (Krause-Kyora et al., 2018a).

Library preparation and sequencing

All DNA extracts were converted into indexed partial Uracil-DNA Glycosylase (UDG) libraries in Kiel using a protocol modified from Rohland et al. (2015) (as described in Krause-Kyora et al., 2018a). Shotgun sequencing was performed on the Illumina HiSeq 4000 (2x75) platform of the IKMB in Kiel.

Metagenomic screening

After using ClipAndMerge v1.7.7 (Peltzer et al., 2016) with default options, the sequencing reads of each sample were screened for the presence of pathogens. MALT v0.4.1 (Vågene et al., 2018) was executed in BlastN mode using a semi-global alignment and a minimum percent identity of 85% to align the samples against a database of 27,730 bacterial and 10,543 viral complete genomes available from the National Center for Biotechnology Information (NCBI) RefSeq database (O'Leary et al., 2016) (January 2019). The results were visualized in MEGAN (Huson et al., 2016). To determine the serovar, reads were aligned to a multi-genome reference including 15 *S. enterica* serovars downloaded from NCBI using BWA v0.7.12 mem (Li, 2013). The number of reads mapping specifically to each genome was retrieved from the BAM files using SAMtools v1.7 idxstats (Li et al., 2009). An endogenous based score was calculated to evaluate the positivity of reads assigned specifically to *S. enterica* and *S.* Paratyphi C using the following formula:

$$\frac{(SP - SE)}{M} \times 1000$$

where SP is the number of reads specifically mapping to *S.* Paratyphi C; SE is the maximum number of reads mapping specifically to any *S. enterica* species with the exception of *S.* Paratyphi C and M is the total number of merged reads in the sample. A score > 0 was identified as *S.* Paratyphi C-positive. In addition, MaltExtract v1.5 from the software package HOPS (Hübler et al., 2019) was used to screen for ancient *Salmonella enterica* and *Yersinia pestis* reads in all samples from this study.

Analysis of *S.* Paratyphi C genome sequences

Samples with more than 300 reads mapping to *S. enterica* were aligned to the reference genome of *S.* Paratyphi C RKS4594 (NC_012125) using BWA mem. DeDup v0.12.2 (Peltzer et al., 2016) was used to remove all duplicate reads from the BAM files and mapDamage v2.0.8 (Jónsson et al., 2013) to evaluate typical aDNA degradation signatures. Genomic variation was identified using Picard Tools v1.139 (http://broadinstitute.github.io/picard) and the Genome Analysis Toolkit (GATK) v3.4.0 (McKenna et al., 2010). The GATK "UnifiedGenotyper" module was used to call reference-based variants from the alignment with default settings and the option "EMIT_ALL_SITES".

Variant effect prediction

VCF files from the three *Salmonella*-positive samples with the highest coverage (HGH-1429, HGH-1558, HGH-1600) were analysed with SnpEff v4.3 (Cingolani et al., 2012) to study effects of variants. The annotated output files were filtered for variants with high impact on the phenotype and researched for their effect.

Phylogenetic reconstruction

Homozygous SNPs were called from a complete dataset of twelve ancient (HGH-1429, HGH-1558, HGH-1600, Ragna (Zhou et al., 2018), Tepos_14 (Vågene et al., 2018), ETR001, OBP001, IKI003, IV3002, MUR009, MUR019, SUA004 (Key et al., 2020)) and 123 modern *S. enterica* subsp. *enterica* genomes (Alikhan et al., 2018; O'Leary et al., 2016; Zhou et al., 2020) versus the reference genome of *S.* Paratyphi C RKS4594 (NC_012125). The MultiVCFAnalyzer v0.87 (Bos et al., 2014) was used with a minimal genotyping quality of 30, minimal base coverage of 5x and minimal allele frequency for homozygous and heterozygous calls of 90%. Variant positions were evaluated in the Integrative Genomics Viewer (IGV) v2.8.2 (Robinson et al., 2011). Positions that

were called in regions of cross-mapping from other organisms and repetitive regions were excluded from the analysis as described previously (Key et al., 2020). The phylogeny was inferred with MrBayes v3.2.7 (Ronquist et al., 2012) using variant-based alignments with a minimal SNP coverage of 5x and 236,622 variant positions. MrBayes was executed with default parameters using the GTR model (lset nst=6 rates=invgamma). The number of simulated generations was increased until the standard deviation of split frequencies was less than 0.01 (mcmc ngen=110,000). Resulting trees were visualized using FigTree (http://tree.bio.ed.ac.uk/software/figtree). Mapping, SNP calling and tree reconstruction were repeated for the reference genome of *S.* Paratyphi A str. AKU_12601 (FM200053.1) to exclude a reference bias and confirm phylogenetic consistency.

Population genetic analyses

Human population genetic analyses were performed as described previously (Krause-Kyora et al., 2018b). Mitochondrial haplogroup assignment was conducted with HaploFind (Vianello et al., 2013) using alignments to the human reference genome *Homo sapiens* hg38 mitochondrial DNA (hg38_chrM).

SUPPLEMENTAL REFERENCES

Alikhan, N.-F., Zhou, Z., Sergeant, M.J. and Achtman, M. (2018). A genomic overview of the population structure of Salmonella. PLoS Genet. *14*, e1007261.

Barta, J.L., Monroe, C., Kemp, B.M. (2013). Further evaluation of the efficacy of contamination removal from bone surfaces. Forensic Sci. Int. *231*, 340–348.

Bos, K.I., Harkins, K.M., Herbig, A., Coscolla, M., Weber, N., Comas, I., Forrest, S.A., Bryant, J.M., Harris, S.R., Schuenemann, V.J., et al. (2014). Pre-Columbian mycobacterial genomes reveal seals as a source of New World human tuberculosis. Nature *514*, 494–497.

Cingolani, P., Platts, A., Le Wang, L., Coon, M., Nguyen, T., Wang, L., Land, S.J., Lu, X. and Ruden, D.M. (2012). A program for annotating and predicting the effects of single nucleotide polymorphisms, SnpEff: SNPs in the genome of Drosophila melanogaster strain w1118; iso-2; iso-3. Fly (Austin) *6*, 80–92.

Cooper, A., Poinar, H. (2000). Ancient DNA. Do It Right or Not at All. Science *289*, 5482.

Fehren-Schmitz, L., Reindel, M., Cagigao, E.T., Hummel, S. and Herrmann, B. (2010). Pre-Columbian population dynamics in coastal southern Peru: A diachronic investigation of mtDNA patterns in the Palpa region by ancient DNA analysis. Am. J. Phys. Anthropol. *141*, 208–221.

Hübler, R., Key, F.M., Warinner, C., Bos, K.I., Krause, J. and Herbig, A. (2019). HOPS: automated detection and authentication of pathogen DNA in archaeological remains. Genome Biol. *20*, 280.

Huson, D.H., Beier, S., Flade, I., Górska, A., El-Hadidi, M., Mitra, S., Ruscheweyh, H.-J. and Tappu, R. (2016). MEGAN Community Edition – Interactive Exploration and Analysis of Large-Scale Microbiome Sequencing Data. PLoS Comput. Biol. *12*, e1004957.

Jónsson, H., Ginolhac, A., Schubert, M., Johnson, P.L.F. and Orlando, L. (2013). mapDamage2.0: fast approximate Bayesian estimates of ancient DNA damage parameters. Bioinformatics *29*, 1682–1684.

Kemp, B.M., Smith, D.G. (2005). Use of bleach to eliminate contaminating DNA from the surface of bones and teeth. Forensic Sci. Int. *154*, 53–61.

Key, F.M., Posth, C., Esquivel-Gomez, L.R., Hübler, R., Spyrou, M.A., Neumann, G.U., Furtwängler, A., Sabin, S., Burri, M., Wissgott, A., et al. (2020). Emergence of human-adapted Salmonella enterica is linked to the Neolithization process. Nat. Ecol. Evol. *4*, 324–333.

Krause-Kyora, B., Nutsua, M., Boehme, L., Pierini, F., Pedersen, D.D., Kornell, S.-C., Drichel, D., Bonazzi, M., Möbus, L., Tarp, P., et al. (2018a). Ancient DNA study reveals HLA susceptibility locus for leprosy in medieval Europeans. Nat. Commun. *9*, 1569.

Krause-Kyora, B., Susat, J., Key, F.M., Kühnert, D., Bosse, E., Immel, A., Rinne, C., Kornell, S.-C., Yepes, D., Franzenburg, S., et al. (2018b). Neolithic and medieval virus genomes reveal complex evolution of hepatitis B. Elife *7*, e36666.

Li, H., Handsaker, B., Wysoker, A., Fennell, T., Ruan, J., Homer, N., Marth, G., Abecasis, G. and Durbin, R. (2009). The Sequence Alignment/Map format and SAMtools. Bioinformatics *25*, 2078–2079.

Li, H. (2013). Aligning sequence reads, clone sequences and assembly contigs with BWA-MEM. arXiv:1303.3997v1.

Lütgert, S.A. (2002). Archäologische Untersuchungen der Massenbestattungen am Heiligen-Geist-Hospital zu Lübeck: Auswertung der Befunde und Funde. In Lübecker Schriften zu Archäologie und Kulturgeschichte 26, M. Gläser, ed. (Rudolf Habelt), pp. 139–243.

McKenna, A., Hanna, M., Banks, E., Sivachenko, A., Cibulskis, K., Kernytsky, A., Garimella, K., Altshuler, D., Gabriel, S., Daly, M., et al. (2010). The Genome Analysis Toolkit: a MapReduce framework for analyzing next-generation DNA sequencing data. Genome Res. *20*, 1297–1303.

O'Leary, N.A., Wright, M.W., Brister, J.R., Ciufo, S., Haddad, D., McVeigh, R., Rajput, B., Robbertse, B., Smith-White, B., Ako-Adjei, D., et al. (2016). Reference sequence (RefSeq) database at NCBI: current status, taxonomic expansion, and functional annotation. Nucleic Acids Res. *44*, D733–45.

Peltzer, A., Jäger, G., Herbig, A., Seitz, A., Kniep, C., Krause, J. and Nieselt, K. (2016). EAGER: efficient ancient genome reconstruction. Genome Biol. *17*, 60.

Prechel, M. (2002). Eine Lübecker Population von 1350 – Krankheiten und Mangelerscheinungen. In Lübecker Schriften zu Archäologie und Kulturgeschichte 26, M. Gläser, ed. (Rudolf Habelt), pp. 245–286.

Robinson, J.T., Thorvaldsdóttir, H., Winckler, W., Guttman, M., Lander, E.S., Getz, G. and Mesirov, J.P. (2011). Integrative genomics viewer. Nat. Biotechnol. *29*, 24–26.

Rohland, N., Harney, E., Mallick, S., Nordenfelt, S., Reich, D. (2015). Partial uracil-DNA-glycosylase treatment for screening of ancient DNA. Philos. Trans. R. Soc. Lond. B. Biol. Sci. *370*, 20130624.

Ronquist, F., Teslenko, M., van der Mark, P., Ayres, D.L., Darling, A., Höhna, S., Larget, B., Liu, L., Suchard, M.A. and Huelsenbeck, J.P. (2012). MrBayes 3.2: efficient Bayesian phylogenetic inference and model choice across a large model space. Syst. Biol. *61*, 539–542.

Vågene, Å.J., Herbig, A., Campana, M.G., Robles García, N.M., Warinner, C., Sabin, S., Spyrou, M.A., Andrades Valtueña, A., Huson, D., Tuross, N., et al. (2018). Salmonella enterica genomes from victims of a major sixteenth-century epidemic in Mexico. Nat. Ecol. Evol. *2*, 520–528.

Vianello, D., Sevini, F., Castellani, G., Lomartire, L., Capri, M. and Franceschi, C. (2013). HAPLOFIND: a new method for high-throughput mtDNA haplogroup assignment. Hum. Mutat. *34*, 1189–1194.

Zhou, Z., Lundstrøm, I., Tran-Dien, A., Duchêne, S., Alikhan, N.-F., Sergeant, M.J., Langridge, G., Fotakis, A.K., Nair, S., Stenøien, H.K., et al. (2018). Pan-genome Analysis of Ancient and Modern Salmonella enterica Demonstrates Genomic Stability of the Invasive Para C Lineage for Millennia. Curr. Biol. *28*, 2420–2428.e10.

Zhou, Z., Alikhan, N.-F., Mohamed, K., Fan, Y. and Achtman, M. (2020). The EnteroBase user's guide, with case studies on Salmonella transmissions, Yersinia pestis phylogeny, and Escherichia core genomic diversity. Genome Res. *30*, 138–152.